Analytic Expressions for Mobilities and Effective Intrinsic Carrier Concentrations in $Ga_{1-x}Al_xAs$ Based on Quantum Mechanical Calculations

Herbert S. Bennett
National Institute of Standards and Technology
herbert.bennett@nist.gov

http://www.eeel.nist.gov/812/itrcs.html
http://www.eeel.nist.gov/812/files/slides1.pdf

15 August 2002

* Identification of products herein does not imply recommendation by NIST, nor does it imply that such products identified are necessarily the best available for the purpose.

OUTLINE

- Motivation
- Carrier Mobilities - Approach and Numerical Results
- Effective Intrinsic Carrier Concentrations - Approach And Numerical Results
- Wireless Application
- Conclusions

MOTIVATION

- **Escalating costs have steadily reduced the number of wafers that can be processed for experimental measurements.**
- **Computer-based experiments/calculations are essential for countering this experimental shortfall.**
- **Basic understanding of many physical phenomena is incomplete.**
- **Predictive computer simulations of processes, devices, and circuits are common critical needs identified in the technology roadmaps from OIDA and NEMI.**

Device Models For GaAlAs

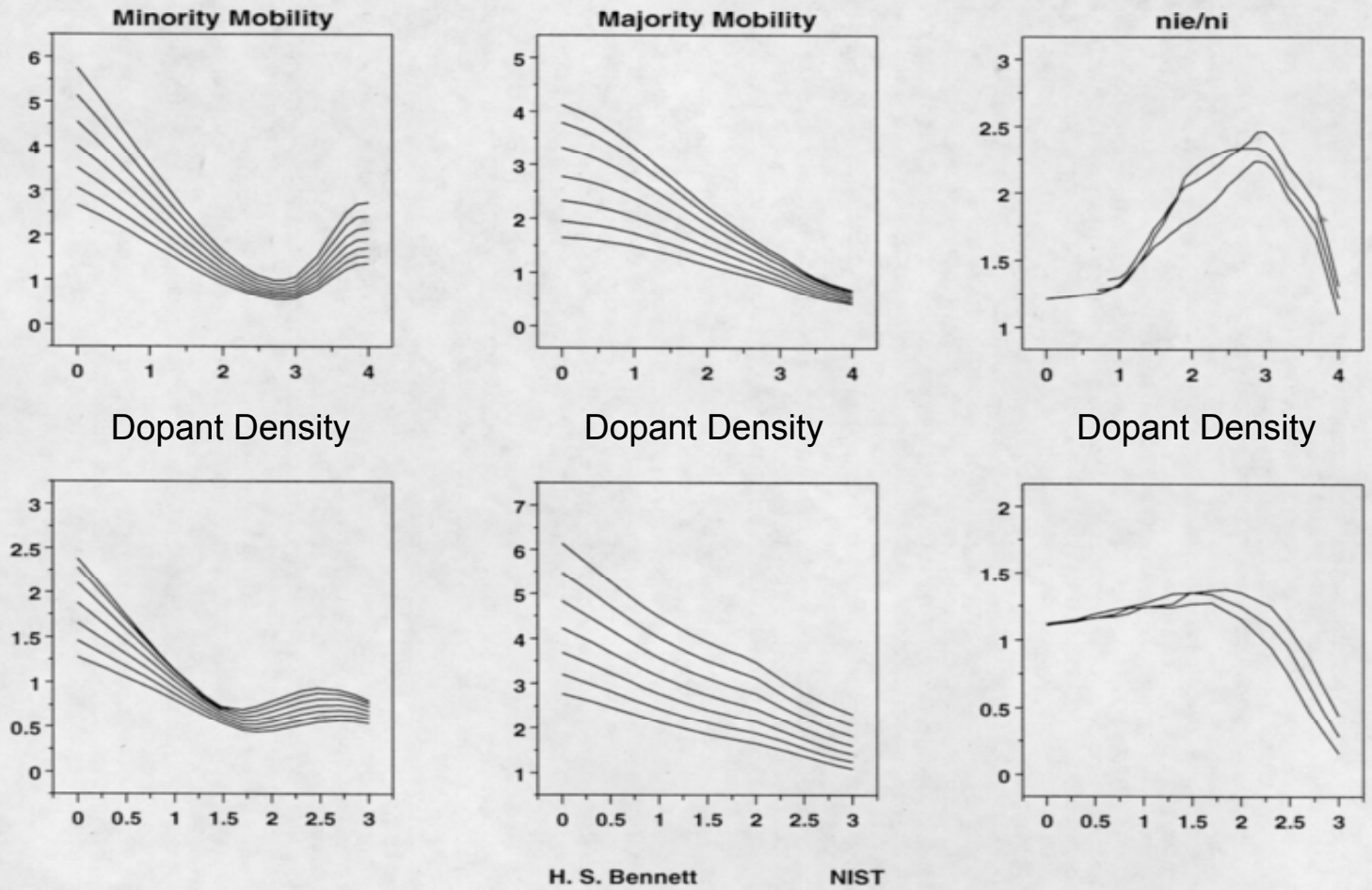

Herbert Bennett, Phone: 301-975-2079

herbert.bennett@nist.gov

9 September 2002

OUTLINE OF TRANSPORT CALCULATIONS

Boltzmann transport equation was solved by a variational procedure that avoids the use of the relaxation-time approximation when it is not valid.

Scattering rates were summed prior to the variational solutions so that Matthiesson's rule is not used.

Phase-shift analysis was used for ionized-impurity and minority carrier-majority carrier scattering so that the Born approximation was not used for these long-ranged or screened scattering potentials.

Scattering rates can be computed as functions of carrier energy for use in Monte Carlo codes.

SCATTERING MECHANISMS

Polar-Optic Phonon Scattering

Non-Polar Optic Phonon Scattering (holes only)

Plasmon Scattering (minority carriers)

Alloy Scattering

Ionized-Impurity Scattering

Carrier-Carrier Scattering

Acoustic Phonon

Piezoelectric Scattering

FROM SUPERCOMPUTER RESULTS FOR A QUANTUM MECHANICAL DESCRIPTION OF CARRIER TRANSPORT - An Example

MINORITY ELECTRON MOBILITY FOR P-TYPE $Ga_{1-m}Al_mAs$ = $\mu_e(p\&type; N_A, m)$

m =	0.00D+00	5.00D-02	1.00D-01	1.50D-01	2.00D-01	2.50D-01	3.00D-01
ACCEPTOR DENSITY	MOBILITY						
CM**-3	CM**2/V.S						
1.00D+16	5.742D+00	5.136D+00	4.552D+00	4.003D+00	3.500D+00	3.051D+00	2.658D+00
2.00D+16	5.106D+00	4.584D+00	4.081D+00	3.606D+00	3.171D+00	2.779D+00	2.434D+00
3.00D+16	4.718D+00	4.244D+00	3.788D+00	3.357D+00	2.961D+00	2.604D+00	2.288D+00
5.00D+16	4.225D+00	3.810D+00	3.411D+00	3.034D+00	2.686D+00	2.371D+00	2.092D+00
7.00D+16	3.903D+00	3.524D+00	3.161D+00	2.818D+00	2.501D+00	2.214D+00	1.959D+00
1.00D+17	3.565D+00	3.224D+00	2.897D+00	2.588D+00	2.303D+00	2.045D+00	1.814D+00
2.00D+17	2.926D+00	2.654D+00	2.394D+00	2.148D+00	1.921D+00	1.715D+00	1.530D+00
3.00D+17	2.569D+00	2.334D+00	2.110D+00	1.899D+00	1.703D+00	1.525D+00	1.366D+00
5.00D+17	2.145D+00	1.953D+00	1.771D+00	1.599D+00	1.441D+00	1.296D+00	1.165D+00
7.00D+17	1.889D+00	1.721D+00	1.564D+00	1.416D+00	1.279D+00	1.154D+00	1.041D+00
1.00D+18	1.643D+00	1.499D+00	1.364D+00	1.239D+00	1.123D+00	1.016D+00	9.198D -01
2.00D+18	1.258D+00	1.150D+00	1.050D+00	9.575D- 01	8.725D -01	7.948D -01	7.241D -01
3.00D+18	1.101D+00	1.006D+00	9.191D -01	8.397D -01	7.670D -01	7.007D -01	6.403D -01
5.00D+18	9.936D -01	9.046D -01	8.249D -01	7.530D -01	6.880D -01	6.292D -01	5.760D -01
7.00D+18	9.901D -01	8.971D -01	8.152D -01	7.420D -01	6.764D -01	6.175D -01	5.647D -01
1.00D+19	1.068D+00	9.601D -01	8.660D -01	7.832D -01	7.097D -01	6.449D -01	5.873D -01
2.00D+19	1.539D+00	1.372D+00	1.227D+00	1.098D+00	9.863D -01	8.881D -01	8.013D -01
3.00D+19	1.964D+00	1.746D+00	1.556D+00	1.390D+00	1.243D+00	1.115D+00	1.002D+00
5.00D+19	2.489D+00	2.212D+00	1.968D+00	1.753D+00	1.563D+00	1.397D+00	1.250D+00
7.00D+19	2.692D+00	2.392D+00	2.125D+00	1.892D+00	1.687D+00	1.506D+00	1.347D+00
1.00D+20	2.720D+00	2.418D+00	2.152D+00	1.918D+00	1.711D+00	1.528D+00	1.368D+00

TO CLOSED FORM ANALYTIC EXPRESSIONS FOR DEVICE SIMULATORS THAN RUN ON ENGINEERING WORKSTATIONS OR CLUSTERS OF SUCH WORKSTATIONS

$$\mu_e(p\&type; N_A, m) = \mu_0 \exp f I(m)$$

$$\% S(m)[w_L(X)g_1(X) \% (1 \& w_L(X))g_2(X)]„$$

where the 147 data points are given in terms of 18 coefficients; namely,

$$I(m) = a_0 \% a_1 m \% a_2 m^2 \% a_3 m^3; \quad S(m) = s_0 \% s_1 m \% s_2 m^2 \% s_3 m^3;$$

$$g_1(X) = c_{10} \% c_{11} X \% c_{12} X^2 \% c_{13} X^3; \quad g_2(X) = c_{20} \% c_{21} X \% c_{22} X^2 \% c_{23} X^3$$

and where $w_L(X) = 1 \& L(X, X_0, \sigma_0)$ and the logistic cumulative distribution function is

$$L(X, X_0, \sigma_0) = 1/f1 \% \exp[\&(X \& X_0)/\sigma_0]„ .$$

A considerable decrease in workstation CPU time for device simulations will occur by using the above analytic expressions instead of interpolating among the 147 data-points in a look-up table.

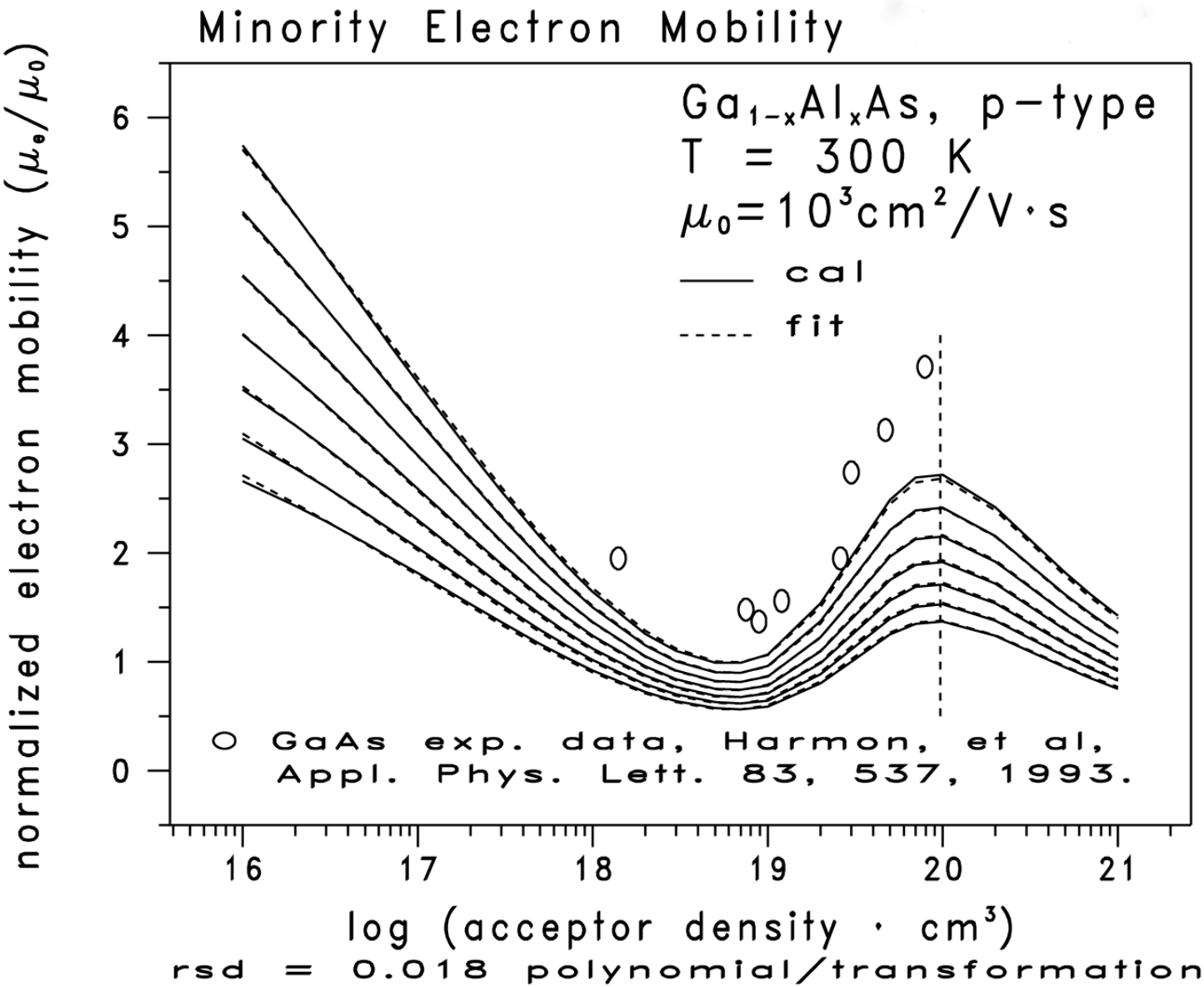
Minority Electron Mobility
$Ga_{1-x}Al_xAs$, p-type
T = 300 K
$\mu_0 = 10^3 cm^2/V \cdot s$
cal
fit
O GaAs exp. data, Harmon, et al,
Appl. Phys. Lett. 83, 537, 1993.
normalized electron mobility (μ_e/μ_0)
0
1
2
3
4
5
6
16
17
18
19
20
21
log (acceptor density · cm^3)
rsd = 0.018 polynomial/transformation

RESULTS

Good agreement has been obtained between these calculations and the experimental majority mobility measurements with no varying of 22 input parameters.

Minority-carrier mobilities are up to three times greater than majority-carrier mobilities.

Phase-shift calculations are needed for ionized-impurity and minority carrier-majority carrier scattering of carriers near band extrema.

Plasmon and carrier-carrier scattering cause a relative minimum in the minority-carrier mobilities as functions of dopant density. This minimum has been verified by experiments. Alloy scattering is not large enough to remove this minimum.

RESULTS

Plasmon scattering has no significant effect on minority hole mobilities.

Applications of these methods to Monte-Carlo calculations should yield more accurate values for velocity-field relations.

I. CARRIER-DOPANT ION INTERACTIONS

KLAUDER FIFTH LEVEL OF APPROXIMATION:

- **Treats two-body interactions to all orders in the scattering potential.**
- **Valid for both low densities with bound and continuum states and high densities with primarily continum states**
- **Self-energy factors for electrons in the presence of a random array of dopant ions**
- **One theory that is valid on both sides of the Mott transition.**

CARRIER-DOPANT ION INTERACTIONS

Klauder's fifth level of approximation for self-energy factors:

$$U_D(\boldsymbol{k},\boldsymbol{q},E) \;=\; N_D v(\boldsymbol{k}-\boldsymbol{q})$$

$$+\int (2\pi)^{-3} d^3\boldsymbol{q}' \; v(\boldsymbol{q}'-\boldsymbol{q}) G(\boldsymbol{q}',E) U_D(\boldsymbol{k},\boldsymbol{q}',E) \;,$$

The Green's function or renormalized propagator:

$$G(\boldsymbol{k},E) \;=\; [E + i\varepsilon - \varepsilon_{\boldsymbol{k}} - \Sigma_D(\boldsymbol{k},E) - \Sigma_A(\boldsymbol{k},E)]^{-1}$$

where $\varepsilon_{\boldsymbol{k}} = \hbar^2 k^2/(2m_e)$, m_e is the effective mass of the electron, $m_e' = (m_e/m_0)$ is the effective mass ratio in terms of the free electron mass, m_0, and $\Sigma_i(\boldsymbol{kK},E) = U_i(\boldsymbol{k},\boldsymbol{k},E)$ is the self-energy with $i = D, A$.

CARRIER-DOPANT ION INTERACTIONS

The spectral density function $A(\boldsymbol{k},E)$ is the wave-vector distribution of the states at energy E

$$A(\boldsymbol{k},E) \;'\; \& \;\pi^{\&1} Im[G(\boldsymbol{k},E)] \;.$$

A broad spectral density of wave-vectors denotes a localized state and a relatively sharply peaked spectral density of wave-vectors denotes a continuum state.

The density of states $\rho(E)$ per unit energy per unit volume

$$\rho(E) \;'\; (2\pi)^{\&3} \int d^3\boldsymbol{k}\; A(\boldsymbol{k},E) \;.$$

$\rho(E)$ occurs in descriptions of electronic, optical, and magnetic propertries.

II. CARRIER-CARRIER INTERACTIONS

- **Theories for the many-body effects of exchange and correlation do not exist for carrier densities between the nondegenerate and degenerate cases in semiconductors at 300 K.**

- **Estimates for exchange (screened exchange term) and correlation (Coulomb hole) energies obtained from the plasmon-pole approximation for the dielectric function with the assumption that the plasmons are not scattered significantly by phonons and impurities;** $\omega_p \tau \gg 1$ **, where** τ **is the scattering time associated with carrier transport and** ω_p **is the plasma frequency,** $\omega_p^2 \; ' \; 4\pi N_D e^2/\varepsilon_0 \kappa m_e$ **.**

III. EFFECTIVE CARRIER CONCENTRATIONS

The electron and hole concentrations at thermal equilibrium:

$$n = \int_{-\infty}^{\infty} f_0(E)\, \rho_c(E)\, dE \quad \text{and} \quad p = \int_{-\infty}^{\infty} [1 - f_0(E)]\, \rho_v(E)\, dE$$

The Fermi-Dirac distribution function:

$$f_0(E) = [1 + \exp\{(E - E_F)/k_B T\}]^{-1} ,$$

where E_F is the Fermi energy, k_B is the Boltzmann constant, and T is the temperature in Kelvin.

EFFECTIVE CARRIER CONCENTRATION

The calculations incorporate the Thomas-Fermi expression for the screening radius:

$$r_s^2 = \frac{4\pi e^2}{\varepsilon_0} \int_{-\infty}^{\infty} \frac{df_0(E)}{dE} [\rho_c(E) - \rho_v(E)]\, dE ,$$

and the charge neutrality condition:

$$N_I = n - p ,$$

And finally, the effective carrier concentration:

$$n_{ie} = (np)^{1/2} .$$

MAJORITY VALENCE BAND DOS Be doped

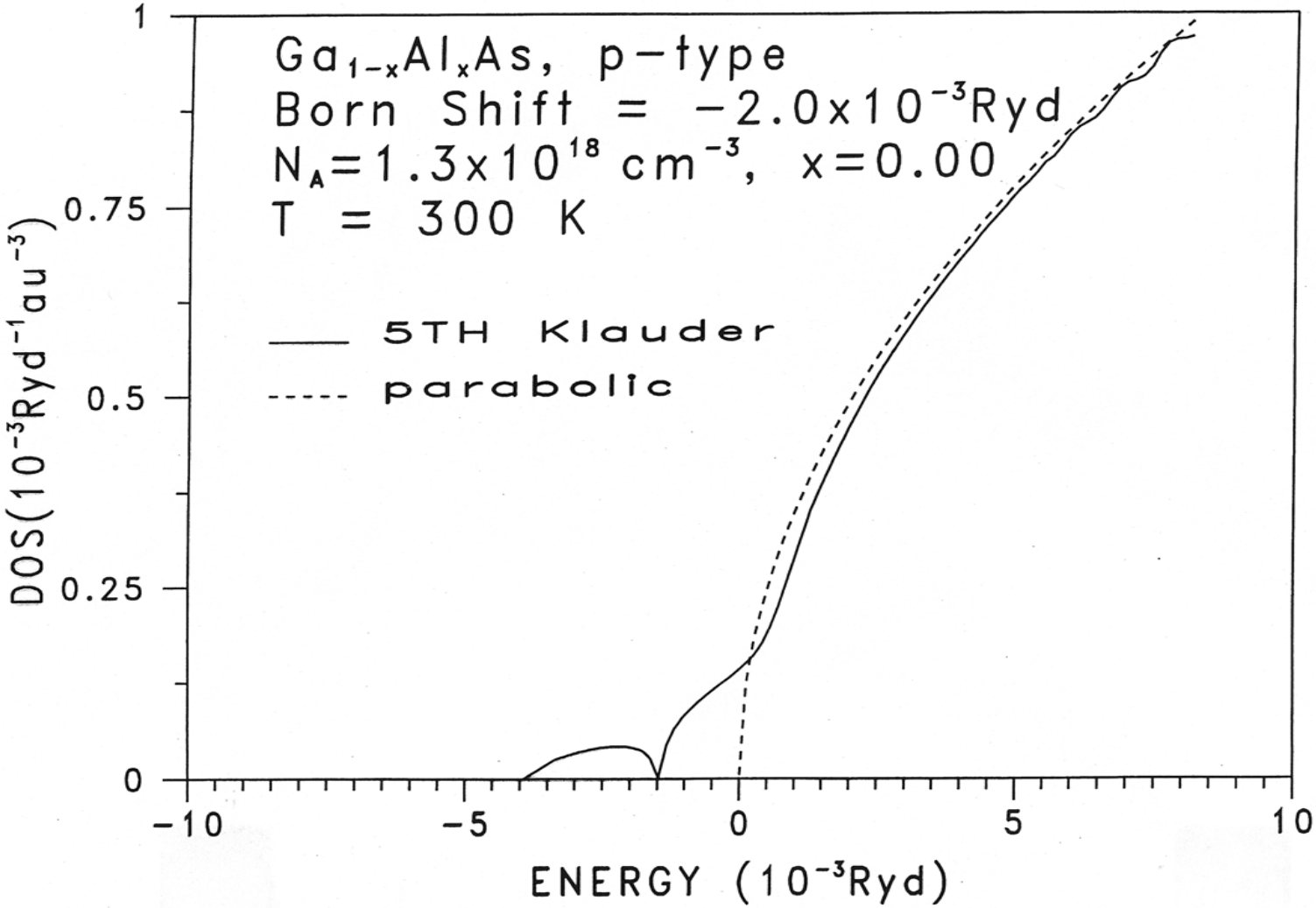

MAJORITY VALENCE BAND DOS Be doped

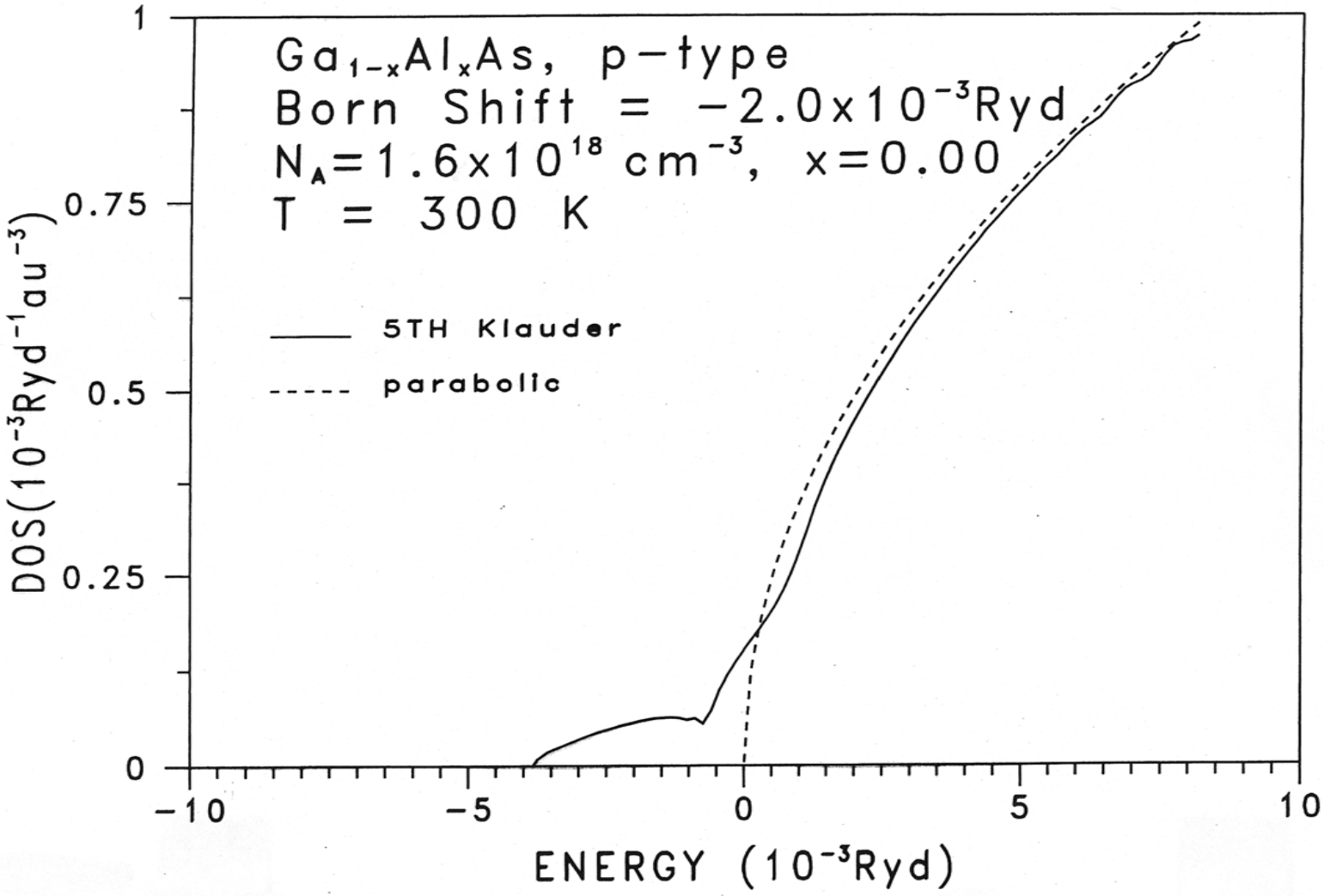

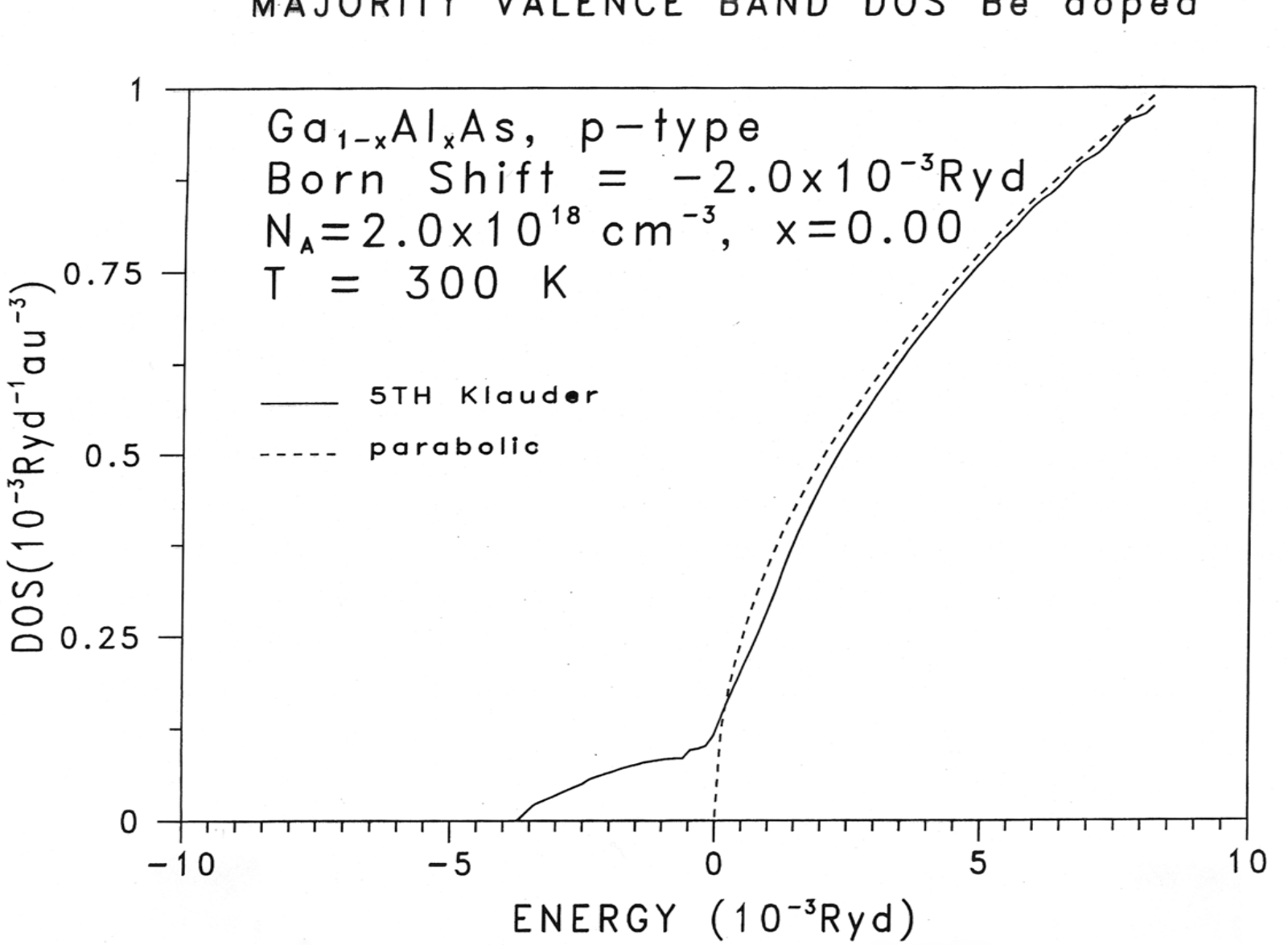
MAJORITY VALENCE BAND DOS Be doped
Ga1-xAlxAs, p-type
Born Shift = −2.0x10−3Ryd
NA=2.0x1018 cm−3, x=0.00
T = 300 K
5TH Klauder
parabolic
DOS(10−3Ryd−1au−3)
1
0.75
0.5
0.25
0
−10
−5
0
5
10
ENERGY (10−3Ryd)

FROM SUPERCOMPUTER RESULTS FOR A QUANTUM MECHANICAL DESCRIPTION OF

EFFECTIVE INTRINSIC CARRIER CONCENTRATION FOR P-TYPE $Ga_{1-x}Al_xAs$

$$n_{ie}(N_A, x) \quad ' \quad (n\,p)^{1/2}$$

NA cm-3	x =	0.00D+00	1.50D-01	3.00D-01
1.00D+16		1.2130	-.--	-.--
2.00D+16		1.2520	-.--	-.--
3.00D+16		1.2130	-.--	-.--
5.00D+16		1.2630	1.2790	-.--
7.00D+16		1.2920	1.3050	1.3610
1.00D+17		1.3270	1.3140	1.4030
1.26D+17		1.3590	1.3280	1.4250
1.58D+17		1.2810	1.3830	1.4060
2.00D+17		1.7860	1.6860	1.4130
2.51D+17		1.3410	1.4340	1.7980
3.00D+17		1.9170	1.6160	1.7170
3.98D+17		1.6700	1.5310	1.7780
5.00D+17		1.7110	2.0640	1.7560
6.31D+17		1.6900	2.1440	2.2950
7.00D+17		1.7230	2.3180	2.3850
7.94D+17		1.9230	2.1820	2.3010
1.00D+18		1.8410	1.9350	2.0880
1.26D+18		1.7740	1.8890	1.9840
1.58D+18		1.7290	2.7970	1.9220
2.00D+18		2.3430	2.4400	1.2630
2.51D+18		1.8800	1.9830	2.0300
3.00D+18		2.1420	2.6200	2.6050
3.98D+18		2.1010	2.4590	2.3890
5.00D+18		2.1570	2.2010	2.3240
6.31D+18		2.1970	2.3240	2.4780
7.00D+18		2.2300	2.3240	2.3290
7.94D+18		2.2210	2.3080	2.4870
1.00D+19		2.2640	2.1820	2.2660
1.26D+19		2.1490	2.2080	2.4210
1.58D+19		2.2250	2.3510	2.5230
2.00D+19		2.0840	2.2000	2.3770
3.00D+19		1.8870	2.0650	2.1870
5.00D+19		1.6470	1.7110	1.8870
7.00D+19		1.3820	1.5260	1.6390
1.00D+20		1.0990	1.2210	1.3160

TO CLOSED FORM ANALYTIC EXPRESSIONS FOR DEVICE SIMULATORS THAN RUN ON ENGINEERING WORKSTATIONS OR CLUSTERS OF SUCH WORKSTATIONS

p-type $Ga_{1-x}Al_xAs$

Nine fitting parameters may be used to represent the 98 calculated data points for the normalized effective intrinsic carrier concentration in p-type $Ga_{1-x}Al_xAs$,
$Y_p = n_{ie}(p\&type; N_A, x)/n_i$, where the donor density is N_A , the mole fraction of AlAs is x , the intrinsic carrier concentration is n_i , and $S_{res}(Y) = 0.205$.

$$Y_p^f(X,x) = A(X) + B(X,x),$$

where

$$A(X) = a_0 + a_1 X + a_2 X^2 + a_3 X^3 + a_4 X^4, \text{ and}$$

$$B(X,x) = (b_0 + b_1 x)/[1 + \{(X - c)/d\}^2] \text{ , and}$$

$$X = \log_{10}(N_A/10^{16} cm^{-3}) .$$

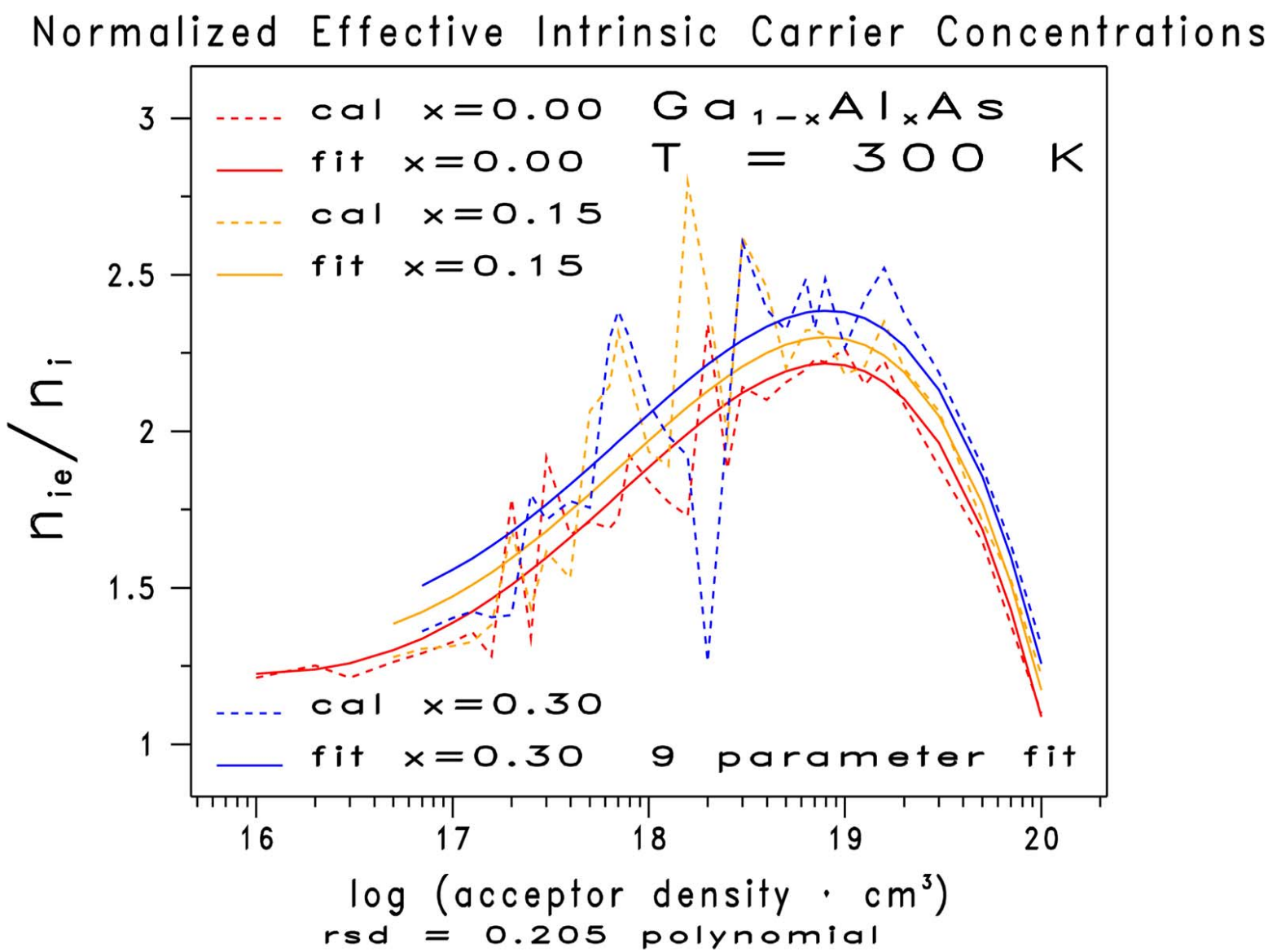
Normalized Effective Intrinsic Carrier Concentrations
cal x=0.00
fit x=0.00
cal x=0.15
fit x=0.15
cal x=0.30
fit x=0.30
Ga1-xAlxAs
T = 300 K
9 parameter fit
nie / ni
3
2.5
2
1.5
1
16
17
18
19
20
log (acceptor density · cm3)
rsd = 0.205 polynomial

Implications for Health Care

Wireless Videophones are Coming

No longer bound to the realm of science fiction, hand-held videophone technology developed at a breakneck pace in late 1999. In Japan, NEC developed a prototype of a small video handset that incorporates a small LCD screen and built-in camera to transmit images and sound simultaneously. And on the other side of the globe, Orange, a UK-based mobile phone firm, has developed a Windows CE-based videophone that receives either Internet-based data or audiovisual information.

The world's first mass-marketed wireless videophone, Kyocera's VisualPhone, broadcasts data at 32Kbps, or about 2 small images per second. Tied closely to the PDA (personal digital assistant) market, handheld internet videophones will become a workable reality in the US only when enough wireless bandwidth becomes available to send and receive a halfway-decent picture—something closer to 400Kbps. NEC's prototype videophone relies on the as-yet undeployed W-CDMA wireless network, which will deliver up to 2000Kbps (2Mbps) when the user is stationary, or about 384Kbps when walking.

Adapted from Videomaker, December 1999, page 13.

3G Spans IEEE Technical Interests

SOURCE: ERICSSON

BY ERICA VONDERHEID
Assistant Editor,
THE INSTITUTE

Third generation wireless (3G) technology promises users more bandwidth, security and reliability. Circuits, antennas, power supply, handheld devices, software and more are employed to develop 3G wireless technology. 3G allows up to 2.05 megabits of data a second to be transferred for stationary applications, 384 Kbits while walking and 128 Kbits for users in moving vehicles.

Spanning several technologies

Because 3G spans many technologies, several IEEE Societies have worked together to spread technical information to other researchers and engineers in the field. These include Antennas and Propagation (A&P), Circuits and Systems (CAS), Communications (ComSoc), Computer (CS), Consumer Electronics (CES), Electron Devices (EDS), Lasers and Electro-Optics, Microwave Theory and Techniques (MTT), Power Electronics Society (PELS), Signal Processing Society (SPS), Solid-State Circuits (SSC) and Vehicular Technology (VTS).

"One can argue that all these (3G wireless) applications fall within the scope of the society," said Stuart Lipoff, a past president of IEEE CES.

Members attend different IEEE meetings and conferences or belong to more than one IEEE society, which leads to collaborative efforts. For example, Lipoff said IEEE CES has worked with IEEE VTS and ComSoc. Lipoff is also a former IEEE VTS Conference Chair.

Often, two or more technical societies and councils will co-sponsor a conference or symposium on a topic. Some examples include

- EDS, MTT – 2001 IEEE Sarnoff Symposium: Advances in Wired and Wireless Communications
- VTS, ComSoc – World Wireless Congress in May in San Francisco
- SSC, EDS – 2002 Custom Integrated Circuits Conference, also in May
- CAS, ComSoc, IEEE Neural Networks Council – IEEE International Conference on Circuits and Systems for Communication this May.

IEEE magazines and journals also play a role in publicizing new wireless technology. Among these are – *IEEE Pervasive Computing, IEEE Transactions on Mobile Computing,* [*Continued on page 9*]

Adapted from The Institute, March 2002, Vol. 26, No. 3, page 1.

A WIRELESS APPLICATION

Results suggest a different design than the one presently used for the $GaAs/Ga_{1-y}Al_yAs$ HBTs used as linear amplifiers.

To increase their operating frequencies, their R_bC_b time constant should be as small as possible and their minority carrier (electron) mobility in the p-type base, $\mu_e(p; N_A)$, should be as large as possible. The base resistance and capacitance are R_b and C_b, respectively.

Most mobility models in current HBT simulators predict that $\mu_e(p; N_A)$ decreases monotonically with increasing N_A, whereas results reported here show that $\mu_e(p; N_A)$ has a relative minimum.

If all other parameters remain essentially the same, then these results suggest that increasing the base doping N_A beyond values used currently in linear HBT amplifiers should increase their operating frequencies because a small range of acceptor densities exists for which the minority mobility increases with increasing acceptor density.

CONCLUSIONS

- **First reported self-consistent calculations from one quantum mechanical theory of bandgap changes, distorted densities of states, and effective carrier concentrations for dopant densities on both sides of and at the Mott transition**

- **These calculations and the recently reported majority and minority electron and hole mobilities now give together an internally self-consistent description of carrier transport in $GaAs/Ga_{1-y}Al_yAs$ heterostructures based on first-principles with no fitting parameters to experimental measurements.**

- **Other ternary or elemental semicondutors may be treated by the same theory at 300 K or temperatures other than 300 K.**

CONCLUSIONS

- **Increased resources for semiconductor materials characterization and model verification are needed to support TCAD applications in industry.**

- **More accurate values for physical parameters are needed in advanced device simulators to reduce the number of unknown physical parameters and to reduce the number of fitting/tuning parameters.**

CONCLUSIONS

1. **Understand problem range of input parameters for which assumptions are valid.**

2. **Know limitations of "first principles calculations."**

3. **Leverage available experimental data to validate and verify physical models.**

CONCLUSIONS

- **Increased resources for semiconductor materials characterization and model verification are needed to support TCAD applications in industry.**

- **More accurate values for physical parameters are needed in advanced device simulators to reduce the number of unknown physical parameters and to reduce the number of fitting/tuning parameters.**